Buckling analysis of composite laminate rectangular and skew plates with various edge support conditions

Chainarin Pannok and Pairod Singhatanadgid

Mechanical Engineering Department, Faculty of Engineering, Chulalongkorn University, Pathumwan, Bangkok 10330, Thailand
Tel: 0-2218-6595, Fax: 0-2252-2889, E-mail: Pairod.S@chula.ac.th

Abstract

This research paper studies the buckling behavior of rectangular and skew thin composite plates with various boundary conditions using the Ritz method along with the proposed out-of-plane displacement functions. The boundary conditions considered in this study are combinations of simple support, clamped support and free edge. The out-of-plane displacement functions in form of trigonometric and hyperbolic functions are determined from the Kantorovich method. In addition to rectangular plates, the proposed method was applied to the skew plates by transforming the domain of skew plate in *x-y* coordinate to a square plate of size 1 unit by 1 unit in the ξ-η coordinate. For rectangular plates with any combination of simple, clamped, and free support, the proposed displacement function yields very good results compared with the available solutions. However, for skew plates, the accurate results are obtained only for plates with clamped support. The solutions of plates with simple support or free support do not have a good convergence. So, the proposed out-of-plane displacement functions can be used to solve the buckling problem of rectangular panels with all combinations of boundary conditions and skew panels with clamped support. Only an approximate solution is obtained if the proposed function is employed to skew plates with simple or free support. Buckling load and modes of specimens with various skew angles and levels of transverse loading are also presented.

Keywords: Buckling, Composite, Rectangular Plate, Skew Plate, Ritz Method

1. Introduction

Recently, composite materials are increasingly used in many mechanical, civil, and aerospace engineering applications due to their high specific stiffness (stiffness per unit density) and high specific strength (strength per unit density). Buckling of composite thin plates is in the interest of many researchers in the past decades. A lot of theoretical and experimental studies are available in the literatures [1-5]. Besides a simple plate configuration such as rectangular plates, several cases of irregular plates are also investigated in many studies. Heitzer and Feuch [6] employed the Rayleigh-Ritz method to analyze the buckling and postbuckling behavior of thin elliptical anisotropic plates. Triangular anisotropic plates were also studied by Jaunky *et al*. [7]. The skew or parallelogram plates which are in the scope of this study were also explored in several studies [8-10]. Most of the studies focused on plates with either simple support or clamped support on all four edges. In this study, the out-of-plane displacement functions for a variety of boundary conditions are employed along with the Ritz method to determine the buckling load and mode of composite laminated plates with a variety of boundary conditions. The buckling behavior of the skew plates are determined and compared to available solutions. The effects of skew angle and transverse tensile loading on the buckling load and mode are also investigated.

2. Problem Statement

This study involves in buckling behavior of rectangular and skew laminated composite plates, as shown in Fig 1. The skew plate can be described by either orthogonal coordinate *x-y* or oblique coordinate ξ-η. The specimen is composed of a number of orthotropic plies with symmetric stacking sequence. The fiber angle θ is measured with respected to the *x*-axis. The skew angle of the specimen α is also measured from the *x*-axis, as shown in the figure. Since a rectangular plate is a special case of skew plates, i.e. in case of α = 90°, all of the derivation in this paper is carried out in form of skew plate configuration. The length of the skewed edges in the ξ and η directions are *a* and *b*, respectively. The specimen is biaxially loaded by in-plane forces in the oblique coordinate system of S_x and S_y. It should be noted that the in-plane forces are in term of force per unit length of plate. In this study, buckling is caused by the in-plane force S_x, which is always a compressive load. The in-plane load in the other direction, S_y, can be either tension or compression. It can be a specified or known load or be a ratio of the unknown buckling load S_x. The boundary conditions of the specimen can be any combinations of the simple support (S), clamped support (C), and free or no support (F).

Besides the oblique loads, the orthogonal in-plane loads N_x, N_y, and N_{xy} are also shown in the figure. These loading will be used later in the Ritz method. The orthogonal loads are also in term of force per unit length.

With a simple derivation using equilibrium equations, the orthogonal in-plane loads are related to the oblique loads as follows;

$$N_x = \left[S_x + S_y \cos^2\alpha\right]/\sin\alpha \tag{1}$$

$$N_y = S_y \sin\alpha \tag{2}$$

$$N_{xy} = S_y \cos\alpha \tag{3}$$

It should be noted that $S_x = N_x$, $S_y = N_y$, and $N_{xy} = 0$ for rectangular plates subjected to biaxial loading.

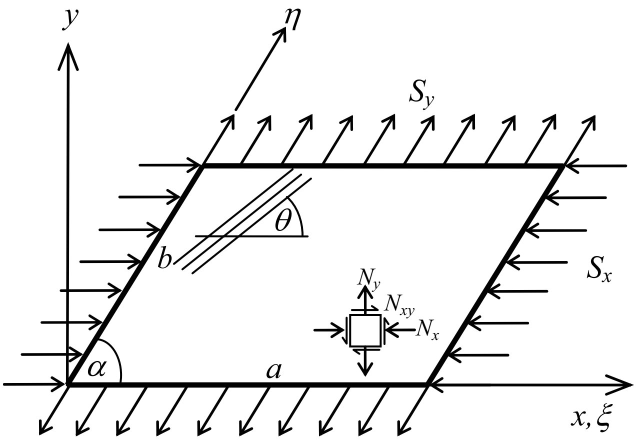

Figure 1. The skew plate with in-plane loading

3. Total Potential Energy Π

To use the Ritz method to determine the buckling load, the total potential energy of the loaded plate must be determined. The total potential energy of the specimen is summation of the strain energy and the potential energy due to the applied loads. For symmetric laminated plate, the total potential energy for a thin composite plate in orthogonal coordinate is written as [3];

$$\Pi = \frac{1}{2}\iint\left\{ D_{11}\left(\frac{\partial^2 w}{\partial x^2}\right)^2 + 2D_{12}\frac{\partial^2 w}{\partial x^2}\frac{\partial^2 w}{\partial y^2} + D_{22}\left(\frac{\partial^2 w}{\partial y^2}\right)^2 + 4D_{16}\frac{\partial^2 w}{\partial x^2}\frac{\partial^2 w}{\partial x \partial y} + 4D_{26}\frac{\partial^2 w}{\partial y^2}\frac{\partial^2 w}{\partial x \partial y} + 4D_{66}\left(\frac{\partial^2 w}{\partial x \partial y}\right)^2 + N_x\left(\frac{\partial w}{\partial x}\right)^2 + N_y\left(\frac{\partial w}{\partial y}\right)^2 + 2N_{xy}\frac{\partial w}{\partial x}\frac{\partial w}{\partial y}\right\} dxdy \tag{4}$$

where D_{ij} is the bending stiffness of the plate
w is the out-of-plane displacement

The out-of-plane displacement function $w(x,y)$ is easier determined for rectangular plate configuration than that of the skew configuration. So, the skew plate configuration is mapped into a unit square as shown in Fig 2. The relationship between the x-y coordinate and the ξ-η coordinate is written as;

$$x = a\xi + (b\cos\alpha)\eta \tag{5a}$$

$$y = (b\sin\alpha)\eta \tag{5b}$$

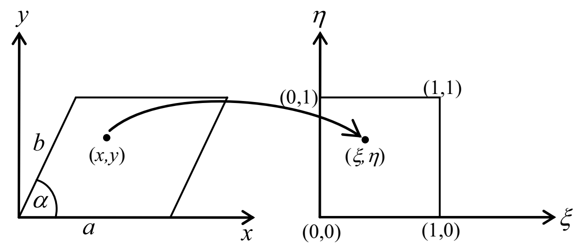

Figure 2. Mapping of the skew plate into a unit square

That is the relationship of an integral of a function in the x-y coordinate is determined in the ξ-η coordinate as;

$$\iint_R f(x,y)dxdy = \iint_R f(x(\xi,\eta), y(\xi,\eta))Jd\xi d\eta \tag{6}$$

where J is the Jacobian matrix defined as;

$$J = \begin{bmatrix} \frac{\partial x}{\partial \xi} & \frac{\partial x}{\partial \eta} \\ \frac{\partial y}{\partial \xi} & \frac{\partial y}{\partial \eta} \end{bmatrix} = \begin{bmatrix} a & b\cos\alpha \\ 0 & b\sin\alpha \end{bmatrix} = ab\sin\alpha \tag{7}$$

So, the total potential energy of the plates in the ξ-η coordinate is simplify to;

$$\Pi = ab\sin\alpha \int_0^1\int_0^1 K_1\left(\frac{\partial^2 w}{\partial \xi^2}\right)^2 + K_2\left(\frac{\partial^2 w}{\partial \xi^2}\frac{\partial^2 w}{\partial \eta^2}\right) + K_3\left(\frac{\partial^2 w}{\partial \eta^2}\right)^2 + K_4\left(\frac{\partial^2 w}{\partial \xi^2}\frac{\partial^2 w}{\partial \xi \partial \eta}\right) + K_5\left(\frac{\partial^2 w}{\partial \eta^2}\frac{\partial^2 w}{\partial \xi \partial \eta}\right) + K_6\left(\frac{\partial^2 w}{\partial \xi \partial \eta}\right)^2 + K_7\left(\frac{\partial w}{\partial \xi}\right)^2 + K_8\left(\frac{\partial w}{\partial \eta}\right)^2 + K_9\left(\frac{\partial w}{\partial \xi}\frac{\partial w}{\partial \eta}\right) d\xi d\eta \tag{8}$$

where;

$$K_1 = \frac{1}{a^4}\left[\frac{D_{11}}{2} + \frac{D_{12}}{\tan^2\alpha} + \frac{D_{22}}{2\tan^4\alpha} - \frac{2D_{16}}{\tan\alpha} - \frac{2D_{26}}{\tan^3\alpha} + \frac{2D_{66}}{\tan^2\alpha}\right]$$

$$K_2 = \frac{1}{b^2\sin^2\alpha}\left(\frac{D_{12}}{a^2} + \frac{D_{22}}{a^2\tan^2\alpha} - \frac{2D_{26}}{a^2\tan\alpha}\right)$$

$$K_3 = \frac{D_{22}}{2b^4\sin^4\alpha}$$

$$K_4 = \frac{2}{a^3 b\sin\alpha}\left(-\frac{D_{12}}{\tan\alpha} - \frac{D_{22}}{\tan^3\alpha} + D_{16} + \frac{3D_{26}}{\tan^2\alpha} - \frac{2D_{66}}{\tan\alpha}\right)$$

$$K_5 = \frac{2}{ab^3\sin^3\alpha}\left(-\frac{D_{22}}{\tan\alpha} + D_{26}\right)$$

$$K_6 = \frac{2}{a^2b^2\sin^2\alpha}\left(\frac{D_{22}}{\tan^2\alpha} - \frac{2D_{26}}{\tan\alpha} + D_{66}\right)$$

$$K_7 = \frac{1}{2a^2}\left(N_x + \frac{N_y}{\tan^2\alpha} - \frac{2N_{xy}}{\tan\alpha}\right)$$

$$K_8 = \frac{N_y}{2b^2\sin^2\alpha}$$

$$K_9 = \frac{1}{ab\sin\alpha}\left(-\frac{N_y}{\tan\alpha} + N_{xy}\right)$$

4. The displacement function

The approximate displacement functions used in this study are written in form of the finite series as;

$$w(\xi,\eta)=\sum_{m=1}^{M}\sum_{n=1}^{N}A_{mn}X_m(\xi)Y_n(\eta) \tag{9}$$

where $X_m(\xi)$ and $Y_n(\eta)$ are the basis functions satisfied the geometric boundary condition of the plate, and A_{mn} are the unknown coefficients to be determined. These basic functions are determined from the solutions of the buckling load of the specially orthotropic plates using the Kantorovich method [11]. Generally, the basis functions are the summation of the trigonometry and hyperbolic functions in form of;

$$\begin{aligned}X_m(\xi)&=A_m\sin p_m\xi+B_m\cos p_m\xi\\&\quad+C_m\sinh q_m\xi+D_m\cosh q_m\xi\end{aligned} \tag{10}$$

This form of function is used for both $X_m(\xi)$ and $Y_n(\eta)$ basis functions. The subscript "*m*" refers to the mode of displacement. The first four modes of the basis function for clamped-free boundary conditions are shown in Fig 3. The boundary conditions are clamped support and free at the left end and right end, respectively.

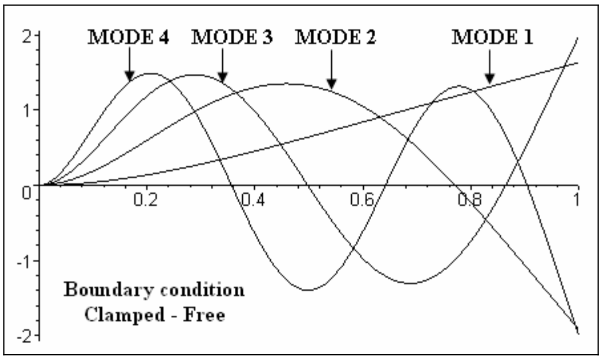

Figure 3. Displacement functions for clamped-free boundary conditions

5. Solution approach

The Ritz method is used in the present study to determine the buckling load and mode of the skew plate. This method begins with obtaining the total potential energy in term of displacement functions by substituting the approximate displacement functions Eq.(9) into the total potential energy, Eq.(8). The displacement functions must be selected such that the geometric boundary conditions of the plate are satisfied. After performing several integrations, the total potential energy is written in term of the undetermined coefficients A_{mn} and the buckling load S_x, given that the transverse load S_y is prescribed or varied with S_x. It is possible to describe to total potential energy in term of the orthogonal loading, but oblique loading is more practical. According to the principle of minimum total potential energy, the total potential energy is minimized with respect to the unknown coefficients A_{mn} according to;

$$\frac{\partial\Pi}{\partial A_{mn}}=0 \tag{11}$$

This procedure gives a system of $M\times N$ linear equations, which can be reduced to a matrix form of generalized eigenvalue problem as

$$[A]\times[C]-S_x[B]\times[C]=0 \tag{12}$$

where [A] and [B] are square matrices whose elements are determined from the plate properties. [C] is a column matrix of an eigenvector, A_{mn}. S_x is the eigenvalue representing the buckling load of the problem. A number of eigenvalues will be obtained after the generalized eigenvalue problem equation, Eq. (12), is solved. The lowest eigenvalue is the buckling load which is of interest. The corresponding eigenvector of that lowest eigenvalue is substituted in the displacement function Eq.(9) to determine the buckling mode.

The convergence study was performed to ensure that the number of term used in the displacement function is enough to give a converged solution. A $[\pm45]_{2S}$ graphite-epoxy rectangular plate is selected for convergence study. The mechanical ply properties of the graphite-epoxy composite are E_{11} = 131 GPa, E_{22} = 10.3 GPa, G_{12} = 6.9 GPa, ν_{12} = 0.22, and ply thickness = 0.127 mm. There are two rectangular plates with aspect ratio of 3, i.e. a = 0.9 m and b = 0.3 m., and the boundary condition of SCCS and CCCC. For SCCS boundary condition, the first letter S and third letter C represent the boundary condition on the ξ = 0 and ξ = 1 edges, respectively. Similarly, the second and fourth letters represent the boundary condition on the η = 0, and η = 1 edges, respectively. The buckling loads of both specimens are determined using different number of terms in the approximate displacement function, Eq.(9). The number of terms used in the convergence study are 1, 4, 9, ..144, i.e. M and N are 1, 2, 3,..12. The buckling loads of both plates are plotted versus the number of terms, as shown in Fig 4. It is seen that the convergence of the buckling load is achieved very well with fairly low number of terms. Thus, in this study, the number of term used in the approximate displacement function is selected as 100, i.e. $M = N = 10$ are used in Eq.(9).

A similar convergence study for skew plate was also performed for both isotropic and composite skew plates. It is found that the convergence of the buckling load is very slow for the specimens with simple support or free edge. For the case of CCCC plates, the buckling load is converged similar to that of the rectangular plate shown in Fig.4. The convergence study for SSSS skew aluminum plate with skew angle of 45° is shown in Fig. 5. A total of 900 terms of the displacement functions, i.e. M=N=30, are used. It is seen that the convergence is very sluggish, even with such a high number of term in the displacement function. So, the proposed functions are not recommended for skew plates with simple support or free boundary conditions.

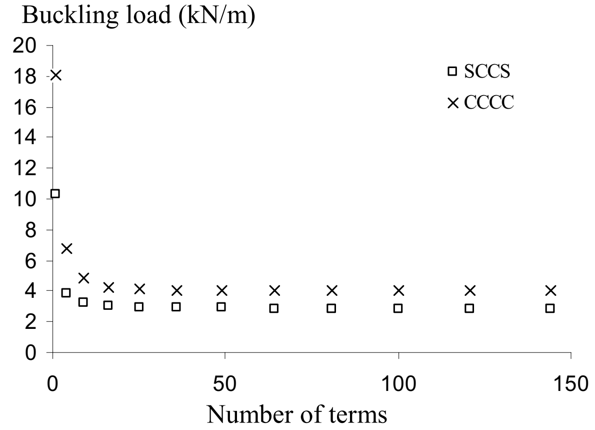

Figure 4. Convergence of the buckling load of $[\pm 45]_{2S}$ rectangular plates

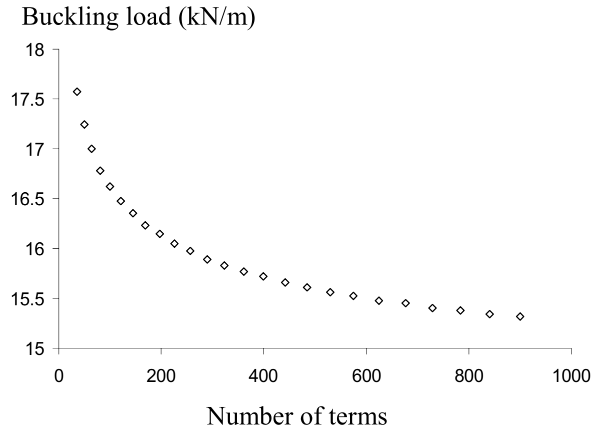

Figure 5. Convergence of the buckling load of aluminum skew plates with skew angle, $\alpha = 45°$

6. Numerical verification

In this section, the buckling loads determined from the proposed displacement functions are verified with the available solutions. Table 1 presents the buckling load of a square composite plate (α = 90°) compared with solutions from other two studies. The boundary conditions of the specimens in this case are CSCS. It can be seen that the differences between buckling loads of the present and past studies are less than one percent. Similarly, buckling loads of $[0/90]_{2s}$ rectangular plates with various combination of boundary conditions are verified with the solution from Kantorovich method [11] in Table 2. The nondimensional buckling load is defined by

$$K_{cr} = \frac{N_x^{cr} b^2}{\pi^2 D_{22}} \tag{13}$$

The boundary conditions are CCCF, SCSF, and SCSC with plate aspect ratios of 1,2, and 3. The buckling loads from this study and the past study match very well with each other.

The solution for skew plate is also compared with the solution from Wang [8] in Table 3. In this comparison, the buckling is initiated by the uniaxial loading with compressive force S_y. To compare with the solutions of the previous study, the obtained buckling loads are transformed to the buckling stress parameter which is defined as;

$$K_{cru} = \frac{S_y b^2}{\pi^2 E_{22} h^3} \tag{14}$$

The material properties of the ply are E_{11}/E_{22} = 10.0, G_{12}/E_{22} =0.5, v_{12} = 0.333, h/b = 0.001. The fiber angles of the specimens are unidirectional of 45°, 60° and 90° with the skew angle of 45° and 60°. The specimens are supported by CCCC boundary conditions. Again, the solutions of the present study are compared very well with those of the previous study.

Table 1. Buckling loads of CSCS square plates compared with the previous studies.

Stacking Sequence	Plate Thickness (in)	Buckling load ($\times 10^3$ lbs)		
		Ref. [11]	Ref. [12]	Present study
$[0/90]_{5S}$	0.115	11.8328	11.7625	11.8312
	0.102	8.2565	8.2074	8.2553
	0.091	5.8630	5.8282	5.8622
$[30]_{20}$	0.110	N/A	9.3453	9.3909
	0.106	N/A	8.3625	8.4149
$[\pm 45]_{2S}$	0.102	N/A	8.3746	8.4230
	0.110	N/A	10.5036	10.5651

Note. E_{11} = 215 GPa (31.18 Msi), E_{22} = 23.6 GPa (3.42 Msi), G_{12} = 5.2 GPa (0.754 Msi), v_{12} = 0.28, $a = b$ = 25.4 cm (10 in.)

Table 2. Nondimensional buckling load factor of $[0/90]_{2s}$ rectangular plates.

B.C.	Method	Aspect ratio, (a/b)		
		1.0	2.0	3.0
CCCF	Ref. [11]	7.8494	2.4895	1.8747
	Present	7.8492	2.4886	1.8737
SCSF	Ref.[11]	2.2294	1.2079	1.3489
	Present	2.2294	1.2089	1.3491
SCSC	Ref. [11]	7.8342	7.3323	7.0500
	Present	7.8342	7.3322	7.0500

Note. $E_{11} = 10E_{22}$, $G_{12} = 0.5E_{22}$, v_{12} = 0.25

In addition to the buckling load, the buckling mode is also determined from the eigenvector corresponding to the lowest eigenvalue. From the eigenvector, the out of plane displacement configuration of the buckled plate in the ξ-η coordinate is determined from Eq.(9). The out-of-plane displacement $w(\xi,\eta)$ is transformed back to that of the x-y coordinate, and then plotted in form of a contour, as shown in Table 4. Each line on the contour represents a line of constant out-of-plane displacement. It is noticed that the buckling mode configuration depends on both fiber angle and skew angle.

Table 3. Buckling stress parameter of skew plates compared with the previous study.

Fiber angle	Skew angle			
	45°		60°	
	Ref. [8]	Present	Ref. [8]	Present study
45°	4.3871	4.3875	3.0507	3.0509
60°	5.4533	5.4544	4.0419	4.0420
90°	4.1062	3.9290	3.9910	3.9927

Table 4. Buckling mode skew composite plates

Fiber angle	Skew angle	
	45°	60°
45°	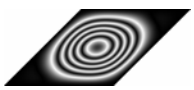	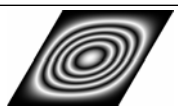
60°	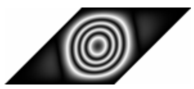	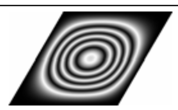
90°		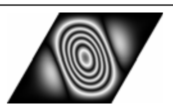

As shown in the convergence study that the convergence in case of simple support is very slow, the buckling loads of an isotropic skew plate with $a/b = 1$ are compared with other studies, as shown in Table 5. The numbers of terms used for the case of SSSS boundary condition are 900 terms. The specimens considered is uniaxially loaded by S_x and the buckling load is presented in term of nondimensional buckling load, Eq.(13). The buckling loads of specimens with CCCC boundary conditions are also presented for comparison. It should be noted that, for CCCC boundary condition, only M=N=10 is used. For case of SSSS boundary condition, the variation of buckling loads from each researcher is fairly high, ranging from 8.47 to 12.30 for skew angle of 45°. Kennedy's solutions are exact solutions since the problem is solved by satisfying the natural boundary conditions. Other solutions used the functions that are not exactly satisfied the natural solutions. In the present study, the double sine series are used as an approximate displacement functions for SSSS boundary conditions, i.e. coefficients B_m, C_m, and D_m are all zero in the displacement functions, Eq.(10). With the double sine series, only the kinematic boundary condition $w = 0$ is satisfied. The force boundary condition $M_n = 0$ (n is a direction normal to the plate boundary) is not satisfied since the proposed function yield the zero moment only in the oblique directions or in direction of ξ and η. In case of CCCC boundary condition, the proposed functions yields zero displacement on the boundary and zero slope in the normal direction, so the obtained buckling load are more accurate and match very well with other studies.

Therefore, the proposed approximate displacement functions are capable of predict the buckling load of rectangular composite plate with various boundary conditions. For skew plates, the proposed function yields an accurate result for only clamped support. Only an approximate solution are obtained for cases of simple or free supports because the force boundary conditions are not satisfied

Table 5. Nondimensional buckling load (K_{cr}) for isotropic skew plates ($a/b = 1$)

B.C.	Solutions	Skew angle (α)			
		90°	75°	60°	45°
SSSS	Durvasula[13]	4.00	4.48	6.41	12.30
	Kennedy [14]	4.00	4.33	5.53	8.47
	Wang [15]	4.00	4.44	6.19	10.60
	Reddy [16]	4.00	4.32	5.55	8.64
	Present	4.00	4.41	6.02	10.70
CCCC	Ashton [17]	-	11.01	13.79	20.67
	Wang [15]	10.08	10.89	13.75	20.69
	Reddy [16]	10.08	10.76	13.64	20.62
	Present	10.07	10.83	13.54	20.13

7. Additional Solution

The buckling loads and modes of $[45]_8$ graphite-epoxy rectangular plates with CCCF, SCSF, and SSCC boundary conditions are presented in Table 6. The specimen aspect ratio is 3; that is the dimensions of the specimen are a = 0.9 m. and b = 0.3 m. The specimens are loaded with either uniaxial loading, i.e. load ratio = 0, or biaxially loading. The buckling is initiated by the compression loading in the x direction, S_x, with tensile load S_y in the other direction. It can be seen that the buckling loads are increased with the applied transverse tensile loading. Similarly, the buckling modes for uniaxial and biaxial loading are different. If the buckling mode is indicated by the number of half-sine curves of the out-of plane displacement. For example, the bucking mode of SSCC plate is increased from mode 4 to mode 5 if the applied transverse tension is half the compressive load. Similar behavior is observed for CCCF and SCSF specimens. If the buckling mode is plotted as a contour plot, the contour will be inclined with respected to the plate boundary because of the inclined fiber angle.

For skew plates, the buckling loads of laminated plates with various skew angles are studied. Buckling loads and buckling modes of graphite-epoxy laminate with stacking sequence of $[0/90]_{2S}$ are shown in Table 7. The boundary condition of the specimens is CCCC with skew angle varied from 75° to 30°. In order to compare the buckling load between each specimen, the area of the plate is kept constant, i.e. the width a and height $b\sin\alpha$ are unchanged for each specimen. In this study, both the width and height of the specimens are 0.3 m. It is found that the buckling load of the specimen with higher skew

Table 6. Buckling loads and modes of $[45]_8$ rectangular plates

Load Ratio	CCCF	SCSF	SSCC
0	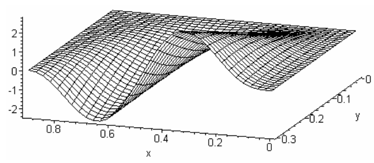 N_x^{cr} = 0.5138 kN/m	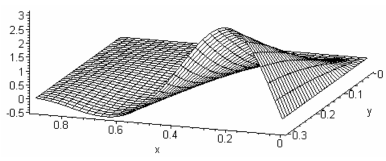 N_x^{cr} = 0.3671 kN/m	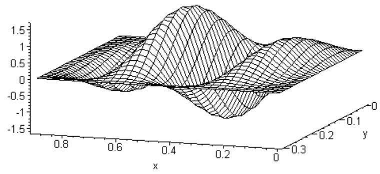 N_x^{cr} = 1.8222 kN/m
-0.5	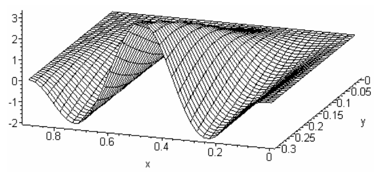 N_x^{cr} = 0.7760 kN/m	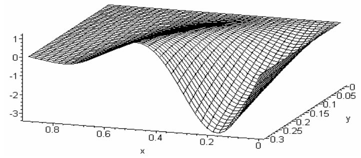 N_x^{cr} = 0.5977 kN/m	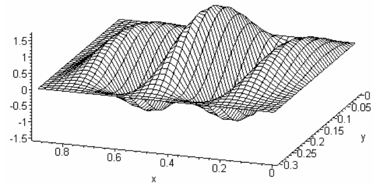 N_x^{cr} = 2.6581 kN/m
-1	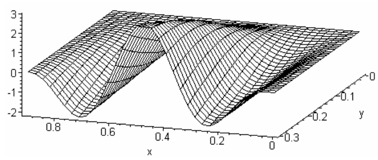 N_x^{cr} = 1.0098 kN/m	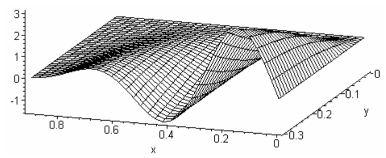 N_x^{cr} = 0.8339 kN/m	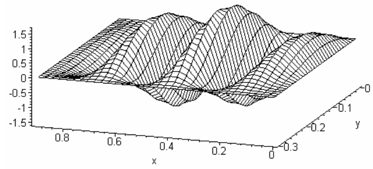 N_x^{cr} = 3.5667 kN/m

angle is higher than that of the lower skew angle. This implies that the rectangular panel has higher load capacity than the skew plate of the same size. For specimens with skew angles of 60° and 75°, the buckling mode is said to be mode 1 since the number of half-sine wave in the direction of the applied load is 1. For specimen with skew angle of 45°, the buckling mode is a little different from other two specimens. There is a small out-of-plane displacement in the corner of the plate. The buckling mode of 30°-skew-angle plate is said to be mode 3 since there are two small contours on the buckled configuration.

Another study involves biaxial loading of the skew composite plates where both S_x and S_y loads are applied simultaneously. The buckling is initiated by the compressive loading S_x while the tensile load S_y is also presented. In this study, the transverse tensile load S_y is assumed to be a ratio of the compressive load S_x. The buckling loads of $[45]_8$ composite plates with boundary conditions of CCCC are presented in Table 8. The specimens are loaded biaxially with the load ratio of 0, -1, and -2, respectively. Similar to the rectangular plates, it can be seen that the buckling load is higher with the applied transverse tension. That is the specimen is reinforced by the transverse tensile loading because the transverse load trends to keep the panel flat. In addition to the buckling loads, buckling modes of the specimens with different load ratio are compared in the third column of the table. The buckling mode is mode 2 for uniaxial loading specimen. The buckling mode changes from mode 2 to mode 3 if the load ratio is increased to load ratio of -2. The buckling mode can be higher than mode 2, i.e. mode 3 or mode 4, if the transverse tensile load is increased.

Table 7. Buckling loads of CCCC $[0/90]_{2S}$ laminates with various skew angle

Skew angle	Buckling Load, S_x (kN/m)	Buckling mode
75°	5.4998	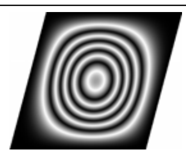
60°	4.9076	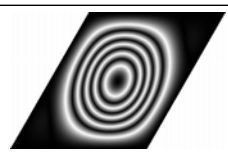
45°	3.9328	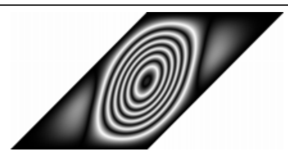
30°	2.6068	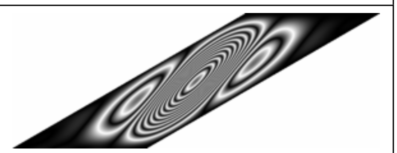

Table 8. Buckling load and mode of $[45]_8$ biaxially-loaded panels

Load Ratio	Buckling Load, S_x (kN/m)	Buckling mode
0	1.791	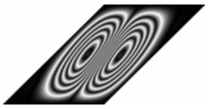
-1	2.376	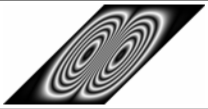
-2	2.924	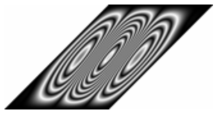

8. Conclusion

In this study, the bucking behavior of rectangular and skew laminate plates with any combinations of simple, clamped, and free boundary conditions is investigated. Both bucking load and buckling mode are examined. The Ritz method along with the proposed approximate out-of-plane displacement functions is adopted. Displacement functions are determined from the buckling problem of a specially orthotropic plate solved by the Kantorovich method. The buckling loads obtained from the present method are verified with the previous studies. A very good agreement between the present solutions and the available solutions is obtained for rectangular plates with any combination of the boundary conditions and the skew plate with CCCC boundary condition. The proposed functions yield only approximate solutions for skew panel with simple support or free boundary condition because the proposed function does not yield the zero moment in the normal direction of the plate's boundary. Addition studies were performed to study the effect of skew angle and the transverse loading to the buckling behaviors. It is found that the buckling load is decreased with the decrease of the skew angle. The buckling mode may change a little bit with the skew angle. For biaxial loading, the buckling load is increase with the magnitude of the transverse tensile loading. The buckling mode may completely change, i.e. mode 2 to mode 3, if the transverse load is high enough.

References

[1] Tung, T. K., and Surdenas, J., 1987. Buckling of rectangular orthotropic plates under biaxial loading. Journal of Composite Materials, Vol. 21, pp.124-128.

[2] Narita, Y., and Leissa, A.W., 1990. Buckling studies for simply supported symmetrically laminated rectangular plates. International Journal of Mechanical Sciences, Vol. 32, pp.909-924.

[3] Chai, G.B., and Hoon, K.H., 1992. Buckling of generally laminated composite plates. Composites Science and Technology, Vol. 45, pp.125-133.

[4] Tuttle, M., Singhatanadgid P., and Hinds, G., 1999. Buckling of Composite Panels Subjected to Biaxial Loading. Experimental Mechanics, Vol. 39, pp.191-201.

[5] Singer, J., Arbocz, J., and Weller, T., 2002. Buckling Experiments: Experimental methods in buckling of thin-walled structures, John Wiley & Sons Inc., New York,

[6] Heitzer, J., and Feuch, M., 1993. Buckling and postbuckling of thin elliptical anisotropic plates. Computers and Structures, Vol. 48, No. 6, pp. 983-992.

[7] Jaunky, N., Knight, Norman F., Jr., and Ambur, D.R., 1995. Buckling analysis of general triangular anisotropic plates using polynomials. AIAA Journal, Vol. 33, No.12, pp.2414-2417.

[8] Wang, S., 1997. Buckling of thin skew fibre-reinforced composite laminates. Thin-Walled Structures, Vol. 28, No. 1, pp. 21-41.

[9] Reddy, A.R. Krishna, and Palaninathan, R., 1995. Buckling of laminated skew plates. Thin-Walled Structures, Vol. 22, No. 4, pp. 241-259.

[10]York, C.B. and Williams, F.W., 1995. Buckling analysis of skew plate assemblies: classical plate theory results incorporating Lagrangian multipliers. Computers and Structures. Vol. 56, No. 4, pp. 625-635.

[11]Ungbhakorn V., and Singhatanadgid P., 2005. Buckling analysis of symmetrically laminated composite plates by the extended Kantorovich method. Composite Structures. Vol. 73, pp.120-128.

[12]Chai GB., 1994. Buckling of generally laminated composite plates with various edge support conditions. Computer and Structures, Vol.29, No.3, pp.299–310.

[13]Durvasula, S., 1971. Buckling of simply supported skew plates. J. Engng Mech. Div., ASCE, Vol 97, No 3, pp.967-979.

[14]Kennedy, J.B., and Prabhakara, M.K.,1978. Buckling of simply supported orthotropic skew plates. Aeronautical Quarterly, Vol.29, pp. 161-174

[15]Wang, C.M., Liew, K.M., and Alwis, W.A.M., 1992. Buckling of skew plates and corner condition for simply supported edges, J. Engng Mech. Div., ASCE, Vol. 118, No 4, pp. 651-662.

[16]Reddy, A.R. Krishna, and Palaninathan, R., 1995. Buckling of laminated skew plates, Thin-Walled Structures, Vol. 22, No 4, pp. 241-259.

[17] Ashton, J.E., 1969. Stability of clamped skew plates under combined loads, Journal of Applied Mechanics, Vol. 36, pp. 139-140.